

# Molecular origin of hardening effect

Weifu Sun\*, Pengwan Chen

State Key Laboratory of Explosion Science and Technology, Beijing Institute of Technology,  
Beijing 100081, P. R. China

\*Corresponding author: E-mail: weifu.sun@bit.edu.cn

DOI: 10.5185/amlett.2019.2187

www.vbripress.com/aml

## Abstract

Hardening effect is often observed in either experiments or simulations. And several continuum models or semi-empirical theories have been proposed to explain the origin, such as constraint-counting theory, the bond-order-length-strength (BOLS) correlation mechanism, equations of state-Murnaghan relationship, etc. However, the validity of these models or theories at the nanoscale have not been tested. In this work, high-speed head-on impact between silicon nanoparticles were studied using molecular dynamics (MD) simulations and their contact mechanics behaviours including contact force versus nominal displacement relationship were explored and the pronounced hardening effect was clearly observed. That's, apparent Young's modulus yielded is much higher than that of their bulk materials. The structure of silicon nanoparticles after compression was analysed in terms of bond length, bond angle, coordination number. The three existing relevant models were separately examined. The results show that any single of the three known theories cannot explain the higher elastic modulus obtained in present MD simulation. Probably, the three aspects contribute together to the hardening effect. This area awaits much more mature theory to explain the hardening effect under the influence of the dynamic effect. Copyright © 2019 VBRI Press.

**Keywords:** Hardening effect, molecular simulation, continuum model.

## Introduction

Significant progress has been achieved in designing and fabricating nanodevices including nano-electro-mechanical systems (NEMS), [1] nanomotors [2] and even molecular machines [3]. The processing and fabrication of such small nanodevices depends on the assembly or self-assembly of the building nanocomponents and the device performance is critically contingent upon the mechanical, electronic, magnetic properties of the building blocks. One of the most important properties is mechanical properties of nanoparticles and state-of-art experimental and numerical technologies have been developed to characterize them, such as interfacial force microscopy, atomic force microscopy (AFM), nanoindentation, etc. Hardening effect, typically the phenomenon that either obtained hardness or elastic modulus of nanoparticles is greater than their bulk counterparts [4-6], has been widely observed from experiments including AFM and nanoindentations, and computer simulations such as molecular dynamics (MD) simulations in particular.

Generally speaking, the extremely high pressures are ascribed to originate from the nanoscale contacts between surface asperities. Numerous experiments and numerical simulations have demonstrated that mechanical properties including hardness, fracture toughness and also effective elastic modulus will be affected when large compressive or tensile stresses develop [5, 7]. For instance, the effective indentation modulus of 100-nm thickened gold films can be enhanced

by 42% subjected to a 50-GPa compressive stress as demonstrated by Jarausch's work [8]. Computational studies on indentation of silicon give rise to a hardness as high as 89 GPa and elastic modulus reaching 397 GPa using quasi-static MD simulation by Astala, *et al.* [6]. Similar phenomenon also occurred to metallic glass under high pressure and compressive pressure of 10 GPa can increase the Young's modulus of glass by 36-40% [9]. However, the driving force behind this hardening effect has not been completely unraveled, although several semi-empirical models or theories have been proposed to explain its origin, such as constraint-counting theory of elastic properties of random networks [10], the bond-order-length-strength (BOLS) correlation mechanism [11], equations of state (EOS)-Murnaghan relationship [5], etc. Inspired by the geophysicists who intensively studied Earth's high pressure inside, EOS has been developed to quantify the influence of pressure on the bulk moduli of materials [5]. Furthermore, whether these models or theories still hold or not at the nanoscale remains largely unknown.

Therefore, in this work, MD simulations will be employed to measure the Young's modulus of silicon nanospheres under high-speed impact and the structural changes after compression including bond angle, bond angle and coordination number etc. will be monitored. The validity of the several models or theories will be tested against MD simulation results.

## Experimental

We carried out the MD simulations following the similar approach as reported elsewhere [12-14]. COMPASS force field [15] was used to describe interactions between the bonded atoms or between non-bond atoms, typically taking the form of Lennard-Jones potential (herein LJ<sup>9-6</sup>) [16]. Briefly, two fully relaxed silicon nanospheres using NVT ensemble at 300 K were put together with certain surface separation distance apart. In a bid to ensure the head-on impact between of two nanospheres along the crystal plane [100] using NVE ensemble, an initially equal but opposite atomic velocity was applied to the X-axis of atoms within the two individual nanospheres whereas zero velocity was assigned to the Y and Z-axis of atoms within the individual nanoparticles. The velocity Verlet integration algorithm was employed with a time step of 1 fs and the frames in the generated trajectory file was output every 100 steps.

## Results and discussion

In this work, contact force  $F_c$  is obtained the following function,<sup>13</sup>

$$F_c = F_n - F_{vdW} - F_{Born} \quad (1)$$

where,  $F_n$ ,  $F_{vdW}$  and  $F_{Born}$  are the normal force, van der waals (vdW) attraction and Born repulsion forces, respectively.

The relationship between elastic restoring force and normal displacement is described by the conventional Hertz model, taking the form of [17].

$$F_c = \frac{4}{3} E^* \sqrt{R^*} \delta_n^{3/2} \quad (2)$$

where,  $1/E^* = (1-\nu_1^2)/E_1 + (1-\nu_2^2)/E_2$ ,  $1/R^* = 1/R_1 + 1/R_2$ , in which  $E$ ,  $\nu$ ,  $R$  and  $\delta_n$  are elastic modulus, Poisson ratio, radius of particle and the normal relative displacement, respectively. Here,  $E=E_1=E_2=130$  GPa,  $\nu=\nu_1=\nu_2=0.28$ <sup>18</sup>,  $R=R_1=R_2$ .

The head-on impact between silicon nanospheres of 2.0 nm in radius at different initial impact velocities of  $V_{i,0} = 200, 1000$  and  $1500$  m/s were conducted and the results are shown in **Fig. 1**. As observed from Fig. 1, it can be seen that at low impact velocity, similar to the silica as reported before [13], the contact force  $F_c$  versus normal displacement  $\delta_n$  relationship obeys the Hertz model well. However, when the initial velocities increases to 1000 m/s, the obtained contact force versus normal displacement relationship exhibit one yield point around  $\delta_n = 0.025$ , indicating that elastic-plastic deformation transition occurs. Prior to the yield point, the contact force versus normal displacement relationship follows the power law of 1.5 as predicted by Hertz model [17], but the yielded elastic modulus by fitting the curve to the Hertz model is much higher than that at 200 m/s. This phenomenon is called hardening effect. After yield point, the force-displacement follows

one linear relationship and this trend conform to the Thornton's model [19] where plastic deformation has appeared.

Now attention will be paid to the apparent Young's modulus obtained at low compression at different initial relative impact velocity of 200 and 1000 m/s. It is known that the Young's modulus of silicon bulk is about 130 GPa along the [100] crystal plane [18]. The yielded Young's modulus by fitting the contact force-normal displacement data to the conventional Hertz model was estimated to be about 497.6 GPa as shown in **Table 1**, which is much higher than that of silicon bulk.

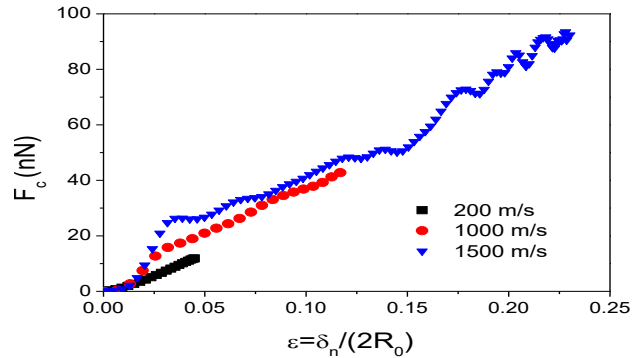


**Fig. 1.** Contact forces versus strain of silicon nanospheres at different initial impact velocities.

Now how come the apparent Young's modulus becomes so higher? Theoretically speaking, three theories or semi-empirical models have been figured out to explain this phenomenon. That is, bond-order-length-strength (BOLS) correlation mechanism, constraint-counting theory pertinent to the elastic properties of random covalent networks, state-Murnaghan relationship.

First, according to the constraint-counting theory, the relationship between Young's modulus and mean atomic coordination  $Z$  is correlated by<sup>10</sup>

$$E = E_0 (Z - 2.4)^{1.5} \quad (3)$$

According to the data in **Fig. 2b**, given the coordination radius is 3.0 Å, the number of atoms corresponding to CN=1, 2, 3, 4, 5, and 6 are 24, 150, 244, 1281, 8 and 2, respectively, thus the mean coordination number is  $Z=3.6465$ . Using Eq. (3), the apparent elastic modulus is about 180.9 GPa, which is still much smaller than 497.6 GPa. The figure on the right indicates the shape change of nanosphere before and after compression.

Second, according to the BOLS correlation mechanism,<sup>11</sup> the change in elastic modulus can be given by

$$\frac{\Delta E}{E_0} = \frac{E - E_0}{E_0} = c_i^{-(m+3)} - 1 \quad (4)$$

where  $m = 4.88$  for silicon,<sup>11</sup>  $c_i$  is the change of bond length between before and after compression. Now take 2 nm-radius silicon nanospheres for instance, the bond length becomes shorten to around 2.20 Å while the

original length is about 2.3516 Å, thus  $c_i=2.2/2.3516\approx 0.9355$ , using Eq. (4), the apparent elastic modulus is about  $E=219.84$  GPa, which is still much smaller than the results obtained from MD simulations of 497.6 GPa (Table 1).

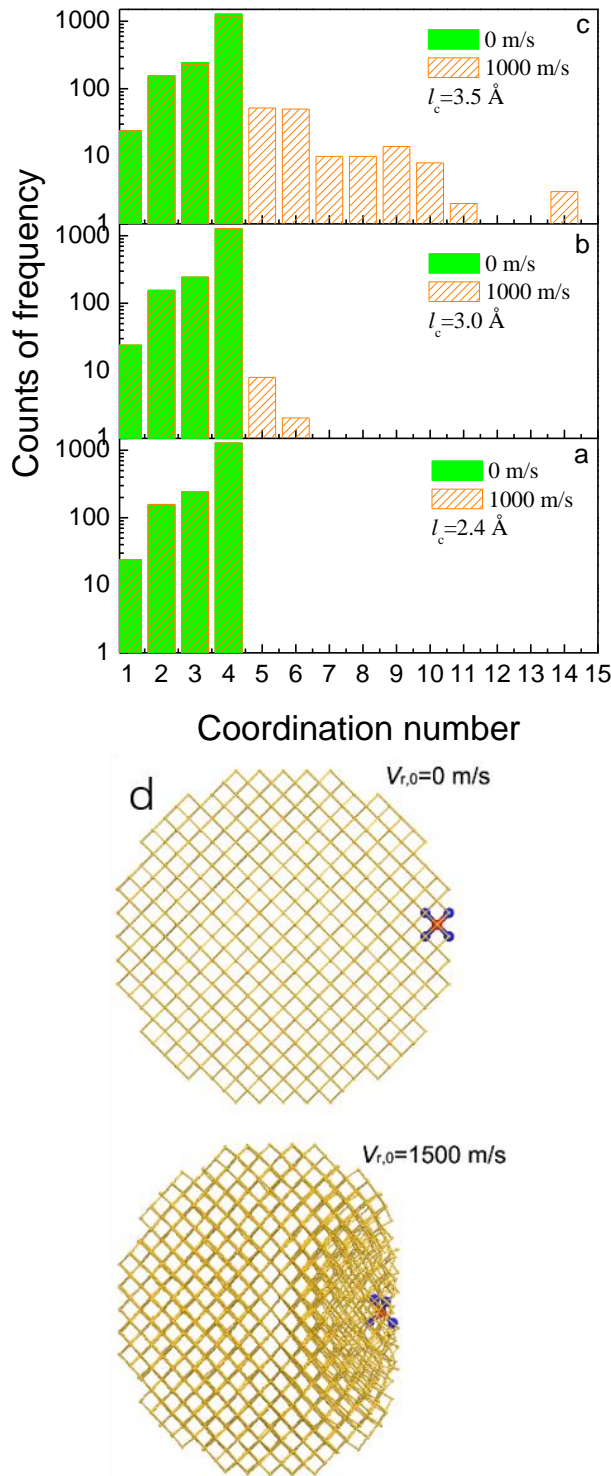


**Fig. 2.** Counts of frequency versus the CN at the maximum compression of 2.0-nm-radius silicon nanosphere at an initial impact velocity of 1000 m/s under the circumstance of coordination radius  $l_c$  at (a) 2.4, (b) 3.0 and (c) 3.5 Å, respectively, and (d) the shape change before and after the maximum compression (In order to highlight the compression effect, 1500 m/s was employed instead of 1000 m/s herein).

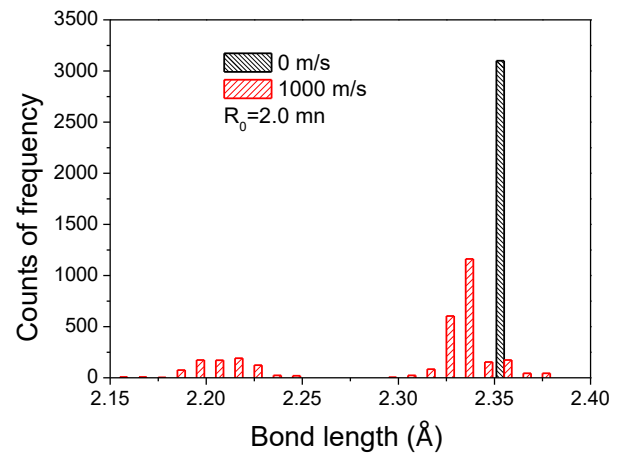


**Fig. 3.** Histograms of counts of frequency versus bond length at the maximum compression of the 2nm-radius silicon nanosphere. Note that 1707 silicon atoms in total.

Thirdly, according to one of the typical equations of state-Murnaghan relationship, the inherent relationship between pressure and elastic modulus  $E$  can be describe by

$$E = E_0 + \beta P_0 \quad (5)$$

where,  $\beta=3\alpha(1-2\nu)$ ,  $P_0$  is the mean contact pressure,  $E_0$  compressive Young's modulus,  $\nu$  is Poisson ratio,  $E_0=130$ GPa,  $\nu=0.28$  [18], a value of  $\alpha=4$  is widely used for a number of materials and particularly silicon.<sup>5</sup>

The particle hardness  $P_0$ , defined as the averaged contact pressure  $P_0$  at the maximum load [20], is evaluated by dividing the maximum load  $F_n^{\text{Max}}$  acting on the nanoparticle by the corresponding contact area [21].

$$P_0 = F_n^{\text{Max}} / \pi (a^*)^2 \quad (6)$$

where,  $a^*$  is the final contact radius.

Contact radius is an important parameter in describing contact behaviors between nanospheres. At the molecular/atomic scale, contact radius can be obtained through the coordinates of atoms within a predefined contact surface. Following the approach of Vergeles *et al.* [22]. The contact radius is given by

$$a^2 = \frac{2}{N_a} \sum_{i=1}^{N_a} \left[ (y_i - Y_{c.m.})^2 + (z_i - Z_{c.m.})^2 \right] \quad (7)$$

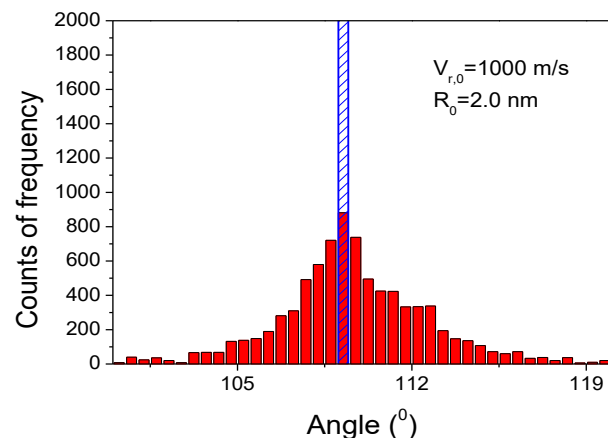
Here  $y_i$  and  $z_i$  are the coordinates of the  $N_a$  atoms within the contact surface,  $Y_{c.m.}$  and  $Z_{c.m.}$  are the centre of mass,  $\sigma=4.45$  Å for silicon atom as obtained from COMPASS forcefield.<sup>15</sup> The contact surface is defined by the  $N_a$  atoms whose  $x$  coordinates lie between  $x_{\text{max}}-0.5\sigma$  and  $x_{\text{max}}$ .

Consequently, the mean contact pressure  $P_0$  at  $V_{r,0}=1000$  m/s is estimated to be about 13.19 GPa, therefore, the apparent elastic modulus  $E$  should be about 199.64 GPa, which is much smaller than 497.6 GPa (Table 1).

**Table 1.** Comparison of apparent Young's modulus (GPa) obtained from MD simulations and estimated from semi-empirical equations.

| Bulk | MD simulations | constraint-counting theory | BOLS  | State-Murnaghan relationship |
|------|----------------|----------------------------|-------|------------------------------|
| 130  | 497.6          | 180.9                      | 219.8 | 199.6                        |

Apart from the coordination number and bond length, the other changes in molecular structure such as bond angle were also measured as displayed in **Fig. 4**. It can be observed that without compression, the bond angle at equilibrium is about  $109.47^\circ$ . However, at the maximum compression after head-on impact at an initial velocity of 1000 m/s, the bond angle distribution develops towards the lower and higher values, both of which deviate further from the equilibrated value of  $109.47^\circ$ . This sheds some light on the high internal pressure within the nanoparticle at the high compression [5].

**Fig. 4.** Histogram of counts of frequency versus angle among the three bonded atoms at the maximum compression of 2.0-nm-radius silicon nanosphere. Note that about 8500 angles and 1707 atoms are included.

In short summary, any single of the three known theories cannot explain the higher elastic modulus obtained in present MD simulation. Probably, the three aspects together contribute to the hardening effect. This area awaits much more mature theory to consider the dynamic effect.

## Conclusion

In this work, the high-speed contact mechanics between silicon nanospheres were explored using MD simulations at initial relative velocity of 1000m/s. The yielded apparent Young's modulus is much higher than silicon bulk counterparts. The molecular structure changes after compression were analysed including bond angle, bond length and coordination number, etc. And the existing three semi-empirical models/theories were tested separately and the results show that any single of the three known theories cannot explain the higher elastic modulus obtained in present MD simulation. Probably, the three aspects contribute together to the hardening effect. This area awaits much

more mature theory to explain the hardening effect under the influence of the dynamic effect.

## Acknowledgements

This work was funded by State Key Laboratory of Explosion Science and Technology (JCRC18-01) and Beijing Institute of Technology Research Fund and the 111 Project (G20012017001).

## Author's contributions

Conceived the plan: Sun, Chen; Performed the experiments: Sun; Data analysis: Sun, Chen; Wrote the paper: Sun, Chen. Authors have no competing financial interests.

## References

- Dai, L.; Zhang, L.; Dong, L. X.; Shen, W. Z.; Zhang, X. B.; Ye, Z. Z.; Nelson, B. J.; *Nanoscale*, **2011**, 3, 4301. DOI: 10.1039/c1nr10650c
- Manesh, K. M.; Campuzano, S.; Gao, W.; Lobo-Castanon, M. J.; Shitanda, I.; Kiantaj, K.; Wang, J.; *Nanoscale*, **2013**, 5, 1310. DOI: 10.1039/c2nr33040g
- Cheng, L. S.; Cao, D. P.; *ACS Nano*, **2011**, 5, 1102. DOI: 10.1021/nn102754g
- Gerberich, W. W.; Mook, W. M.; Perrey, C. R.; Carter, C. B.; Baskes, M. I.; Mukherjee, R.; Gidwani, A.; Heberlein, J.; McMurry, P. H.; Girshick, S. L.; *J. Mech. Phys. Solids*, **2003**, 51, 979. DOI: 10.1016/s0022-5096(03)00018-8
- Mook, W. M.; Nowak, J. D.; Perrey, C. R.; Carter, C. B.; Mukherjee, R.; Girshick, S. L.; McMurry, P. H.; Gerberich, W. W.; *Phys. Rev. B*, **2007**, 75, 214112. DOI: 10.1103/PhysRevB.75.214112
- Astala, R.; Kaukonen, M.; Nieminen, R. M.; Heine, T.; *Phys. Rev. B*, **2000**, 61, 2973. DOI: 10.1103/PhysRevB.61.2973
- Wen, Y. H.; Wang, Q.; Liew, K. M.; Zhu, Z. Z.; *Phys. Lett. A*, **2010**, 374, 2949. DOI: 10.1016/j.physleta.2010.05.015
- Jarusch, K. F.; Kiely, J. D.; Houston, J. E.; Russell, P. E.; *J. Mater. Res.*, **2000**, 15, 1693. DOI: 10.1557/jmr.2000.0244
- Wang, W. K.; *Mater. Trans.*, **2001**, 42, 606. DOI: 10.2320/matertrans.42.606
- He, H.; Thorpe, M. F.; *Phys. Rev. Lett.*, **1985**, 54, 2107. DOI: 10.1103/PhysRevLett.54.2107
- Sun, C. Q.; *Prog. Solid State Chem.*, **2007**, 35, 1. DOI: 10.1016/j.progsolidstchem.2006.03.001
- Sun, W. F.; Zeng, Q. H.; Yu, A. B.; *Langmuir*, **2013**, 29, 2175. DOI: 10.1021/la305156s
- Sun, W. F.; Zeng, Q. H.; Yu, A. B.; Kendall, K.; *Langmuir*, **2013**, 29, 7825. DOI: 10.1021/la401087j
- Sun, W. F.; *Nanoscale*, **2013**, 5, 12658. DOI: 10.1039/c3nr04354a
- Sun, H.; *J. Phys. Chem. B*, **1998**, 102, 7338. DOI: 10.1021/jp980939v
- Rappe, A. K.; Casewit, C. J.; Colwell, K. S.; Goddard, W. A.; Skiff, W. M.; *J. Am. Chem. Soc.*, **1992**, 114, 10024. DOI: 10.1021/ja00051a040
- Hertz, H.; *J. Reine Angew. Math.*, **1882**, 92, 156.
- Hopcroft, M. A.; Nix, W. D.; Kenny, T. W.; *J. Microelectromech. Syst.*, **2010**, 19, 229. DOI: 10.1109/jmems.2009.2039697
- Thornton, C.; Ning, Z. M.; *Powder Technol.*, **1998**, 99, 154. DOI: 10.1016/j.powtec.2011.01.013
- Valentini, P.; Gerberich, W. W.; Dumitrica, T.; *Phys. Rev. Lett.*, **2007**, 99, 175701. DOI: 10.1103/PhysRevLett.99.175701
- Johnson, K. L.; *Contact mechanics*. 2nd ed.; Cambridge University Press: Cambridge, **1985**, 84.
- Vergeles, M.; Maritan, A.; Koplik, J.; Banavar, J. R.; *Phys. Rev. E*, **1997**, 56, 2626. DOI: 10.1103/PhysRevE.56.2626